ARTICLE

Validation of Broadband Infrared Normalization in Sum-Frequency Generation Vibrational Spectroscopy through Simultaneous Chiral Terms on α-Quartz Crystal†

Jia-Jie Li[a,b‡], Wei-Wang Zeng[b,c‡], Wen Zeng[b,c], Qiong Zeng[a,b], Chuanyao Zhou[b], Xueming Yang[b,d], Zefeng Ren[a,b*]

a. Department of Chemical Physics, University of Science and Technology of China, Hefei 230026, China
b. State Key Laboratory of Molecular Reaction Dynamics, Dalian Institute of Chemical Physics, Chinese Academy of Sciences, Dalian 116023, China
c. University of Chinese Academy of Sciences, Beijing 100049, China
d. Department of Chemistry, Southern University of Science and Technology, Shenzhen 518055, China

(Dated: Received on March 8, 2023; Accepted on April 18, 2023)

Sum-frequency generation vibrational spectroscopy (SFG-VS) has been widely used for characterizing various interfaces. However, obtaining SFG signals with a high signal-to-noise ratio can be challenging for certain interfaces, such as those involving powder particles, which scatter the SFG light and make it difficult to obtain accurate spectra. To address these challenges, we developed a new approach using a z-cut α-quartz crystal as the substrate loaded with a very small amount of powder sample. This approach not only amplifies the SFG signal from particles through the interference of the electric field from the quartz crystal, but also allows for phase reference and normalization of the broadband infrared SFG spectrum. By distinguishing the different polarizations of the SFG light, we were able to separate and simultaneously collect the achiral and chiral SFG signals. We used the chiral SFG signal to normalize the achiral SFG intensity, thereby avoiding any potential changes to the interface caused by loading substances onto the quartz, as well as coincidence differences resulting from the instability of light at different moments. We demonstrated our method by measuring the adsorption of CH_3OD on a quartz substrate loaded with MoC nanoparticles. Our approach produced a high signal-to-noise ratio SFG spectrum, regardless of the interface situation.

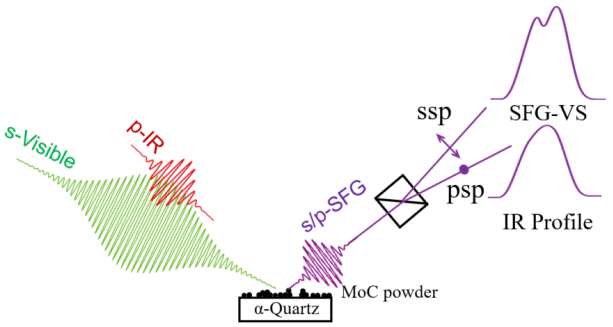

Key words: α-Quartz, Broadband IR, Normalization, Methanol, Powder, MoC, Sum-frequency generation vibrational spectroscopy

I. INTRODUCTION

Sum-frequency generation vibrational spectroscopy (SFG-VS) has proven to be an effective spectroscopic tool on surface and interface research [1−3]. As a second-order nonlinear optical process, it possesses intrinsic interface-selectivity and is forbidden in the centrosymmetric media under the dipole approximation

†Part of the special topic for "the Chinese Chemical Society's 17th National Chemical Dynamics Symposium"
‡These authors contributed equally to this work.
*Author to whom correspondence should be addressed. E-mail: zfren@dicp.ac.cn

[4−7]. This important feature makes SFG-VS intrinsically interface-selective. Over the years, it has been extensively used to study the molecular structures and dynamics of various surface such as liquids, heterogeneous catalysis, and biology [8−13]. As a purely optical characterization method, SFG-VS can detect all the buried interface and without the interference of bulk molecules, as long as they are accessible by light [14, 15]. Therefore, it is a powerful tool for studying interfacial processes in catalysis even under the high-pressure gas atmospheres [16−21]. However, most of the early studies focus on the single crystal model catalytic system rather than practical powder catalysts. This is largely due to the significant scattering of the detection light by the powder catalysts, which results in weak and difficult-to-collect surface SFG signals [22, 23].

To reduce the scattering of incident lights and SFG by the powder particle, we have successfully achieved the SFG measurements by loading a very small amount of powder on a quartz substrate [20]. This method has two advantages, one of which is that a small amount of powder still allows the light to be dominated by reflection rather than scattering, so reflective SFG experimental configuration is still suitable. In addition, by utilizing the interference between the bulk non-resonant SFG signal from the quartz substrate and the SFG signal from adsorbed molecules on the particle surface, the resonant SFG signal of the surface can be enhanced [24]. The simplicity and feasibility of this method can significantly improve the signal-to-noise ratio of SFG spectra and have been demonstrated by studying the adsorption behavior of CO on Pt nanoparticles [20]. However, it is still difficult to detect the weaker signals, such as reaction intermediates and trace products. We believe that the challenge of increasing the signal-to-noise ratio remains in accurately normalizing the obtained SFG spectra. The current measurement techniques for SFG fall into two categories: scanning infrared (IR) wavelengths [25, 26] and broadband IR [27, 28]. Normalization is necessary because the IR light has different intensities for different wavelengths, especially for broadband SFG which has a broad intensity distribution as a function of IR wavelength. The common approach for normalizing SFG signals involves using the reference standard materials, such as GaAs [29], Au [30] or quartz [24]. In our previous works, SFG spectra were normalized by the combination of SFG signals with an azimuthal offset of 60° or 180° on a z-cut quartz crystal [31, 32]. This normalization method is often applicable in cases where the quartz surface has a uniform interface, such as with a uniform adsorption or coating. However, normalization may be more challenging in cases where the surface adsorption and substrate is not uniform, such as particles-loaded substrates. The non-uniformity of the particles on substrates leads to the differences in the coincidence of input light beams on the surface, resulting in a decrease of the signal-to-noise ratio and artificial features of the spectrum. Therefore, increasing the accuracy of the normalization method is an essential process for the detection of weak signals from powder particles.

Here, we have developed a novel method to normalize broadband IR SFG spectrum using a z-cut α quartz crystal as a substrate. This approach allows for the simultaneous collection of chiral and achiral SFG signals using a single optical path. The chiral signal on the z-cut α-quartz crystal typically originates only from the bulk and does not contain information about surface molecules. Additionally, both chiral and achiral SFG can be generated simultaneously by the same incident light beams at the same position on the sample. As a result, this method allows for monitoring spot coincidence, scattering, and pulse energy fluctuations of the two incident light beams. This method provides us a highly reliable and effective means of normalizing broadband IR SFG spectrum [25, 33, 34].

II. PRINCIPLE OF NORMALIZING BROADBAND IR WITH α-QUARTZ CRYSTAL

z-cut α-quartz crystal has been widely used as intensity and phase standard in SFG measurements because it is spectroscopically flat in a broad spectral range from UV to mid-IR due to its nonresonance [35−39]. It is also often used in external heterodyne phase-resolved (EHPR) measurements [40, 41]. Recently, Wang *et al.* has developed internal heterodyne phase-resolved (IHPR) measurements by using two special properties of the z-cut α-quartz crystal: the intrinsic $\pi/2$ shift of the bulk contribution versus the surface contribution to the SFG field and the 3-fold azimuthal angle structural phase dependence of the quartz crystal with a D_3 symmetry [24, 39]. The IHPR method does not require multiple measurements like the EHPR method and only requires one measurement, and there is no phase shift. However, the IHPR method can only be used for specific surfaces in contact with the phase reference interface. The total SFG signal on α-quartz crystal is composed

DOI:10.1063/1674-0068/cjcp2303020

of the bulk contribution of the quartz crystal within the coherent length and the surface contributions from the adsorbed layer [24, 42]. The intensity of SFG is given by [43]

$$I_{\mathrm{SFG}} \propto \left|\chi_{\mathrm{eff}}^{(2)}\right|^2 I_{\mathrm{Vis}}\left(\omega_{\mathrm{Vis}}\right) \cdot I_{\mathrm{IR}}\left(\omega_{\mathrm{IR}}\right) \tag{1}$$

where $I_{\mathrm{Vis}}(\omega_{\mathrm{Vis}})$ and $I_{\mathrm{IR}}(\omega_{\mathrm{IR}})$ are the intensities of the visible and IR light, respectively, and $\chi_{\mathrm{eff}}^{(2)}$ is the effective second-order nonlinear susceptibility tensor. In IHPR measurements [24],

$$\begin{aligned}\left|\chi_{\mathrm{eff}}^{(2)}\right|^2 &= \left|\chi_{\mathrm{S,Re}}^{(2)} + i\chi_{\mathrm{S,Im}}^{(2)} + i\chi_{\mathrm{Q}}^{(2)}\right|^2 \\ &= \left|\chi_{\mathrm{Q}}^{(2)}\right|^2 + 2\chi_{\mathrm{Q}}^{(2)} \cdot \chi_{\mathrm{S,Im}}^{(2)} + \left|\chi_{\mathrm{S}}^{(2)}\right|^2 \end{aligned} \tag{2}$$

Here, $\chi_{\mathrm{Q}}^{(2)}$ is the second-order nonlinear susceptibility of the quartz crystal, off-resonant from UV to mid-IR, $\chi_{\mathrm{S}}^{(2)}$ is the second-order nonlinear susceptibility of the adsorbed layer, and $\chi_{\mathrm{S,Im}}^{(2)}$ is its imaginary part. In general, the first term is much larger than the third one, so the third item can be omitted [24, 39]. And thus

$$\left|\chi_{\mathrm{eff}}^{(2)}\right|^2 \approx \left|\chi_{\mathrm{Q}}^{(2)}\right|^2 + 2\chi_{\mathrm{Q}}^{(2)} \cdot \chi_{\mathrm{S,Im}}^{(2)} \tag{3}$$

Due to that the D_3 symmetry of quartz results in the phase dependence with a three-fold azimuthal angle, the $\chi_{\mathrm{Q}}^{(2)}$ term changes sign when rotating z-cut α-quartz crystal by 60° or 180°, whereas the $\chi_{\mathrm{S,Im}}^{(2)}$ term remains the same sign due to its isotropic on surface [24]. Therefore, through SFG measurements with rotating the quartz crystal and simple algebraic operations, Wang *et al.* developed the measurements of imaginary spectrum [39], followed by our work to develop the imaginary spectrum under high-pressure gas environments [31]. In these works, the SFG spectra are normalized to the SFG signal from z-cut α-quartz crystal (proportional to $|\chi_{\mathrm{Q}}^{(2)}|^2$) by another measurement on a clean z-cut α-quartz crystal surface or based on two times of measurements with rotating angles difference 60° or 180° of the z-cut α-quartz crystal [31]. To obtain a high-quality spectrum, it requires the stable laser power and IR spectrum in the two measurements, and the overlapping conditions of the two beams to be the same. However, there are two more troublesome problems for the particles sample loaded on a flat surface. One is that the uniform distribution of the particle on a flat surface is very tricky, and the other is that the scattering from the particle is evitable.

On z-cut α-quartz crystal, both the achiral susceptibility terms, corresponding to macroscopical terms ssp, ppp, sps, pss, sss, and chiral susceptibility terms, corresponding to macroscopical terms psp, spp, pps, are dominant. Additionally, the maximum macroscopically achiral and chiral terms responding to azimuthal rotating angle are all 30° shifted between ssp and psp, ppp and psp, sps and pps [39]. Here we take the example of simultaneous measurements of ssp and psp. Since the surface is isotropic, the $\chi_{\mathrm{S,Im}}^{(2)}$ with psp term is zero if the adsorbed molecules are achiral. Hence, the ssp and psp SFG signals are

$$\begin{aligned} I_{\mathrm{ssp}} \propto & \left(\left|\chi_{\mathrm{Q,ssp}}^{(2)}\right|^2 + 2\chi_{\mathrm{Q,\,ssp}}^{(2)} \cdot \chi_{\mathrm{S,Im}}^{(2)}\right) \\ & \cdot I_{\mathrm{Vis}}\left(\omega_{\mathrm{Vis}}\right) I_{\mathrm{IR}}\left(\omega_{\mathrm{IR}}\right) \end{aligned} \tag{4}$$

$$I_{\mathrm{psp}} \propto \left|\chi_{\mathrm{Q,psp}}^{(2)}\right|^2 I_{\mathrm{Vis}}\left(\omega_{\mathrm{Vis}}\right) \cdot I_{\mathrm{IR}}\left(\omega_{\mathrm{IR}}\right) \tag{5}$$

The I_{psp} reflects the IR spectral profile. Then, we can obtain the normalized ssp spectrum, $I_{\mathrm{ssp,norm}}$, by dividing Eq.(4) by Eq.(5) as

$$\begin{aligned} I_{\mathrm{ssp,\,norm}} &= \frac{I_{\mathrm{ssp}}}{I_{\mathrm{psp}}} = \frac{\left|\chi_{\mathrm{eff,ssp}}^{(2)}\right|^2}{\left|\chi_{\mathrm{eff,psp}}^{(2)}\right|^2} \\ &\approx \frac{\left|\chi_{\mathrm{Q,ssp}}^{(2)}\right|^2 + 2\chi_{\mathrm{Q,ssp}}^{(2)} \cdot \chi_{\mathrm{S,Im,ssp}}^{(2)}}{\left|\chi_{\mathrm{Q,psp}}^{(2)}\right|^2} \\ &= c^2 + 2c\frac{\chi_{\mathrm{S,Im,ssp}}^{(2)}}{\chi_{\mathrm{Q,psp}}^{(2)}} \end{aligned} \tag{6}$$

where $c=\dfrac{\chi_{\mathrm{Q,ssp}}^{(2)}}{\chi_{\mathrm{Q,psp}}^{(2)}}$. Simultaneously obtaining SFG signals with both ssp and psp polarization combinations not only reduces data acquisition time but also eliminates the impact of laser instability on the signal-to-noise ratio (SNR). This method automatically removes the influence of gas-phase IR absorption on the normalized spectrum under gas environments. Importantly, it can eliminate inhomogeneity of the particles sample distribution on surface, and the effect of particles on light scattering. To improve the SNR of the normalized spectrum, we can rotate the azimuthal angle of z-cut α-quartz crystal to get about the same value between $|\chi_{\mathrm{Q,ssp}}^{(2)}|^2$ and $|\chi_{\mathrm{Q,psp}}^{(2)}|^2$. And thus,

$$I_{\mathrm{ssp,\,norm}} \approx 1 + \frac{2\chi_{\mathrm{S,Im,ssp}}^{(2)}}{\chi_{\mathrm{Q,psp}}^{(2)}} \tag{7}$$

DOI:10.1063/1674-0068/cjcp2303020

III. EXPERIMENTAL METHODS

A. Sample preparation

The z-cut α-quartz crystal (size, 16 mm×2 mm, obtained from Bright Crystals Technology, Inc.) was carefully prepared. The crystal was cleaned using a plasma cleaner (Tergeo Basic, PIE Scientific LLC) with air as the gas source. The cleaning conditions were set to a RF power of 75 W, a treatment time of 5 min, and an air pressure greater than 25 Pa in the treatment chamber. To load the crystal with the MoC powder particles from Ma group [44], we prepared the samples by dispersing the particles in deionized water, allowing big particles to settle, then taking the upper layer and diluting it again. After another settling step, we took the upper layer and drop it (∼30 μL) onto the quartz substrate. The excess solution was removed using a vacuum pump, resulting in a thin layer of MoC nanoparticles on an area of approximately 100 mm^2. Obvious unevenness and aggregation can be seen. Surface scattering is mainly caused by the aggregation of particles into larger clumps. Methanol (CH_3OD, ≥99.9%, Sigma-Aldrich) was purified by undergoing several freeze-pump-thaw cycles prior to use in the experiment.

B. SFG experiments

The experimental setup for broadband IR SFG measurements and a homemade sample cell was described in detail elsewhere [20, 45]. In brief, a femtosecond regenerative amplifier (Legend Elite Duo HE-USP, Coherent, Inc.) generated 40 fs pulses with 3.2 mJ/pulse, at the repetition rate of 5 kHz and a central wavelength of 800 nm. About 2.2 mJ was used to pump an optical parametric amplifier and non-collinear difference frequency generator to generate a tunable mid-IR beam in a potassium titanyl arsenate (KTA) crystal. A picosecond regenerative amplifier (Legend Elite Duo HE-P, Coherent, Inc.), which shared the same seed from a Ti:sapphire oscillator (Vitara-T HP, Coherent Inc.) generated about 1 ps pulse with 3 mJ/pulse. And then it passed through an air-spaced etalon (SLS OPTICS Ltd.) to generate a spectrally narrowed picosecond beam (about 2.6 cm^{-1} FWHM) used as the visible (Vis) light. The SFG was generated by focusing the VIS and the IR beam on the sample surface with both temporal and spatial overlap. The incident angles of VIS and IR were 43° and 55° with respect to the surface normal, respectively. To conduct the SFG measurement, a z-cut α-quartz crystal loaded with MoC nanoparticles was placed in a homemade cell, and the crystal temperature can be heated by CO_2 laser. The SFG signal reflected from the sample surface was collimated by an achromatic lens. To achieve the simultaneous measurements of achiral and chiral SFG terms (ssp and psp in this work), a Wollaston prism was used to separate s- and p-polarized SFG light by 1.5° in the vertical plane. A linear polarizer at an angle of 45° was placed before the focusing lens incident on the monochromator, which was used to maintain the same transmission in the monochromator and the same quantum efficiency of CCD for the s- and p- polarized lights as shown in FIG. 1 (a) and (b). FIG. 1(c) shows two separated SFG signals were distributed vertically on the CCD. Two regions of interest (ROI) can be selected and accumulated. The signal was tilted on the CCD arising from the spatial chirp of IR light in the vertical direction. Simultaneous SFG measurement of multiple polarization combination has been successfully applied in several groups. Smits *et al.* used a displacing prism and a pair of cylindrical lenses to separate the s- and p- SFG signals [46], while Tan *et al.* used a pair of Glan-Laser polarizers to separate the s- and p- SFG signals [47, 48]. Compared with these two methods, our method using a Wollaston prism is simpler.

IV. EXPERIMENTAL RESULTS

Molybdenum carbide (MoC) is a well-known catalyst utilized in water-gas reaction and aqueous-phase reforming of methanol, and it has been extensively investigated [44, 49]. However, the presence of defects in the material causes strong absorption in the visible to infrared range, which makes it challenging to obtain the vibrational spectrum of adsorbates on its surface. In this work, we employed MoC nanoparticles loaded on a z-cut α-quartz crystal to validate our proposed method for normalizing the infrared spectral profile of broadband IR SFG.

Two different normalization methods were used: the SFG spectrum obtained from the bared z-cut α-quartz crystal surface and the chiral SFG spectrum. The untreated MoC nanoparticles were loaded onto the crystal, the SFG spectra were obtained under vacuum conditions after exposure to 10 kPa CH_3OD vapor, followed by evacuation. FIG. 2(a) shows the original ssp SFG vibrational spectra from two different positions on the crystal surface (black and red lines) and the IR spectral

DOI:10.1063/1674-0068/cjcp2303020

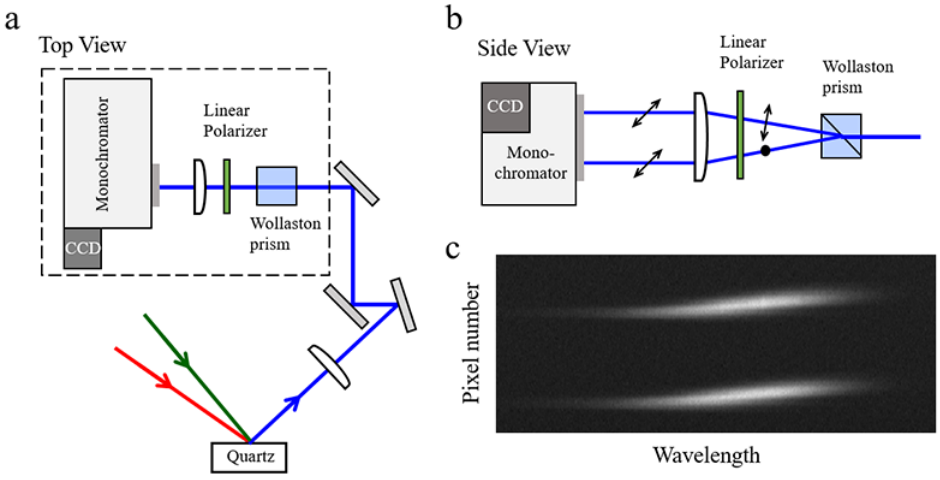

FIG. 1 Top (a) and side (b) views of SFG collection optical path. Both s- and p-polarized SFG signals generated on the z-cut α-quartz crystal with loaded MoC nanoparticles are collimated by an achromatic lens, separated by a Wollaston prism by 1.5° in the vertical plane, and repolarized at 45° with a linear polarizer. (c) Two separated SFG signals distributed vertically on the CCD.

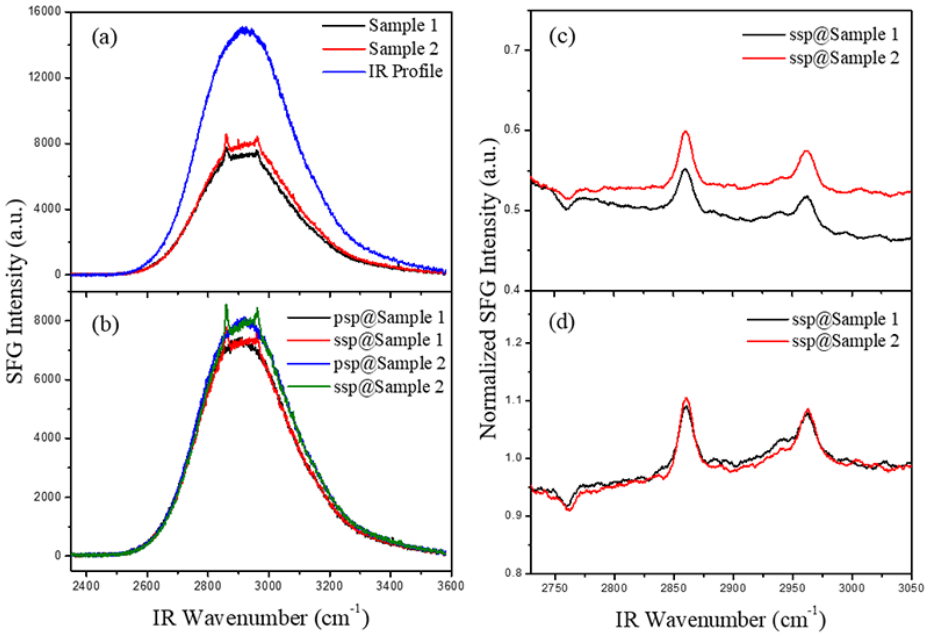

FIG. 2 (a) Original ssp-SFG spectra on two different positions (black and red lines) on z-cut α-quartz crystal surface with MoC nanoparticles and IR spectral profile (blue line) on the clean crystal surface. (b) Original ssp- (red and olive lines) and psp- (black and blue lines) SFG spectra on two different positions on the crystal surface with MoC. SFG spectra (c) normalized by the IR spectral profile on the clean quartz surface in (a), and SFG spectra (d) normalized by psp-SFG spectra in (b). Experimental data of (c) and (d) were smoothed by adjacent-averaging 11 points.

profile obtained from a clean position (blue lines). In the original spectra, two features are observed in the C−H stretching range. The SFG signal is significantly reduced due to absorptions from the MoC nanoparticles and scattering from the aggregated nanoparticles. Moreover, both SFG spectra are not consistent with each other, and there is an obvious overall shift. This problem would become more prominent if the loaded nanoparticles were thicker. FIG. 2(c) shows SFG vibrational spectra obtained from both positions after normalization by the IR spectral profile. We can find that the SFG spectrum on position 2 looks better than that on position 1, which is obviously tilt. The peaks at 2758, 2860 and 2960 cm^{-1} are assigned to OD stretch,

DOI:10.1063/1674-0068/cjcp2303020

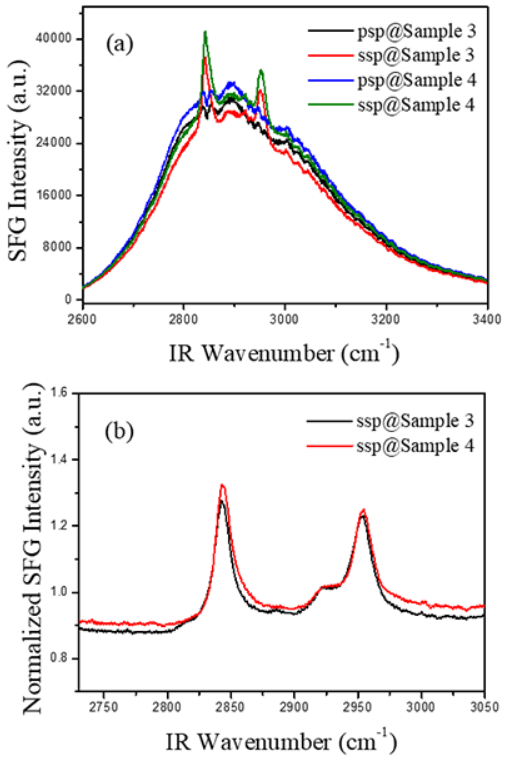

FIG. 3 (a) Original ssp- (red and olive lines) and psp- (black and blue lines) SFG spectra on two different positions on the z-cut α-quartz crystal loaded with MoC nanoparticles under 10 kPa CH_3OD pressure in the cell. (b) SFG spectra normalized by psp-SFG spectra in (a). Experimental data of (b) were smoothed by adjacent-averaging 5 points.

the symmetric stretching vibration, and the Fermi resonances of CH_3 group of methoxy on quartz [31, 50]. The small feature at 2940 cm^{-1} is from the hydrocarbon contaminants on MoC nanoparticles. FIG. 2(b) shows the achiral ssp-SFG spectra and the chiral psp-SFG spectra on the sample from the two positions on the sample. The ssp-SFG spectra from the two positions are not consistent with each other due to different distribution of MoC nanoparticles on the surface. However, when the SFG spectra are normalized using the chiral term of psp- SFG spectrum, the spectra obtained from the two positions show almost the same features, as shown in FIG. 2(d). The vibrational spectrum of methoxy on MoC is only observed by pretreating MoC under high temperature, which will be reported in our further work.

FIG. 3 shows both the original and normalized SFG spectra obtained under the 10 kPa CH_3OH pressure in the cell. The original SFG spectra, as shown in FIG. 3(a), clearly reveal IR absorption from the gas phase, as well as the physisorption of CH_3OH on the quartz crystal surface. The peaks observed at 2843, 2923, and 2953 cm^{-1} were assigned to the symmetric stretching vibration and two Fermi resonances of CH_3 group of methanol on the quartz crystal surface, as previously reported in literuateres [31, 50]. The features from chemisorption of CH_3OH, methoxy, are much weaker than those from physisorption, and can not be resolved. Furthermore, FIG. 3 also shows that the non-uniform distribution of MoC nanoparticles on the surface, resulting in inconsistent SFG intensities at different positions and varying surface nonresonance intensities. Despite this, the normalized SFG spectra exhibit a high SNR, and the characteristic peaks of the adsorbed molecules are discernible at coincident positions.

V. CONCLUSION

In summary, we have developed a novel method to normalize broadband IR SFG spectra, which we have successfully demonstrated methanol on a z-cut α-quartz crystal loaded with MoC nanoparticles as a model system. Our approach's feasibility and reliability are verified by comparing the SFG-VS normalized by the SFG obtained from clean quartz with that normalized by simultaneously measuring the chiral SFG signal on quartz. Additionally, we have confirmed the universality of our method by collecting SFG signals under gas environments. This work represents a significant advancement in our ability to obtain vibrational spectra on powder samples in gas environments, and it has great potential in deepening our understanding of real catalytic reactions.

VI. ACKNOWLEDGMENTS

This work was supported by Ministry of Science and Technology of China (No.2018YFA0208700), the National Natural Science Foundation of China (No.21688102). We thank the group of professor Ding Ma from Peking University to provide us the MoC nanoparticle sample.

[1] Y. R. Shen, Nature **337**, 519 (1989).
[2] K. B. Eisenthal, Chem. Rev. **96**, 1343 (1996).
[3] C. S. Tian and Y. R. Shen, Surf. Sci. Rep. **69**, 105 (2014).
[4] F. M. Geiger, Annu. Rev. Phys. Chem. **60**, 61 (2009).
[5] Y. R. Shen, *Fundamentals of Sum-Frequency Spectroscopy*, Cambridge: Cambridge University Press, (2016).

DOI:10.1063/1674-0068/cjcp2303020

[6] P. A. Covert, W. R. FitzGerald, and D. K. Hore, J. Chem. Phys. **137**, 014201 (2012).
[7] R. R. Feng, A. A. Liu, S. Liu, J. Shi, Y. Liu, and Z. Ren, Chin. J. Chem. Phys. **28**, 11 (2015).
[8] A. Ghosh, B. B. Hsu, S. M. Dougal, M. Afeworki, P. A. Stevens, and M. S. Yeganeh, ACS Catal. **4**, 1964 (2014).
[9] R. R. Feng, A. A. Liu, S. Liu, J. Shi, R. Zhang, and Z. Ren, J. Phys. Chem. C **119**, 9798 (2015).
[10] X. Peng, R. Zhang, R. R. Feng, A. A. Liu, C. Zhou, Q. Guo, X. Yang, Y. Jiang, and Z. Ren, J. Phys. Chem. C **123**, 13789 (2019).
[11] M. R. Watry and G. L. Richmond, J. Phys. Chem. B **106**, 12517 (2002).
[12] K. Engelhardt, W. Peukert, and B. Braunschweig, Curr. Opin. Colloid Interface Sci. **19**, 207 (2014).
[13] K. Strunge, F. Madzharova, F. Jensen, T. Weidner, and Y. Nagata, J. Phys. Chem. B **126**, 8571 (2022).
[14] C. T. Williams and D. A. Beattie, Surf. Sci. **500**, 545 (2002).
[15] S. Ye, K. T. Nguyen, S. V. L. Clair, and Z. Chen, J. Struct. Biol. **168**, 61 (2009).
[16] C. Klünker, M. Balden, S. Lehwald, and W. Daum, Surf. Sci. **360**, 104 (1996).
[17] H. Härle, A. Lehnert, U. Metka, H. R. Volpp, L. Willms, and J. Wolfrum, Chem. Phys. Lett. **293**, 26 (1998).
[18] A. Bandara, S. Dobashi, J. Kubota, K. Onda, A. Wada, K. Domen, C. Hirose, and S. S. Kano, Surf. Sci. **387**, 312 (1997).
[19] M. S. Yeganeh, S. M. Dougal, and B. G. Silbernagel, Langmuir **22**, 637 (2006).
[20] T. Luo, R. Zhang, X. Peng, X. Liu, C. Zhou, X. Yang, and Z. Ren, Surf. Sci. **689**, 121459 (2019).
[21] T. Dellwig, G. Rupprechter, H. Unterhalt, and H. Freund, Phys. Rev. Lett. **85**, 776 (2000).
[22] S. Roke, W. G. Roeterdink, J. E. G. J. Wijnhoven, A. V. Petukhov, A. W. Kleyn, and M. Bonn, Phys. Rev. Lett. **91**, 258302 (2003).
[23] A. G. F. de Beer, S. Roke, and J. I. Dadap, J. Opt. Soc. Am. B **28**, 1374 (2011).
[24] L. Fu, S. L. Chen, and H. F. Wang, J. Phys. Chem. B **120**, 1579 (2016).
[25] N. Ji, V. Ostroverkhov, C. Y. Chen, and Y. R. Shen, J. Am. Chem. Soc. **129**, 10056 (2007).
[26] S. Yamaguchi and T. Tahara, J. Chem. Phys. **129**, 101102 (2008).
[27] K. I. Inoue, T. Ishiyama, S. Nihonyanagi, S. Yamaguchi, A. Morita, and T. Tahara, J. Phys. Chem. L **7**, 1811 (2016).
[28] L. J. Richter, T. P. Petralli-Mallow, and J. C. Stephenson, Opt. Lett. **23**, 1594 (1998).
[29] C. Y. Tang and H. C. Allen, J. Phys. Chem. A **113**, 7383 (2009).
[30] J. F. D. Liljeblad and E. Tyrode, J. Phys. Chem. C **116**, 22893 (2012).
[31] T. Luo, R. Zhang, W. W. Zeng, C. Zhou, X. Yang, and Z. Ren, J. Phys. Chem. C **125**, 8638 (2021).
[32] T. Luo, W. W. Zeng, R. Zhang, C. Zhou, X. Yang, and Z. Ren, ACS Appl. Electron. Mater. **3**, 1691 (2021).
[33] J. Wang, P. J. Bisson, J. M. Marmolejos, and M. J. Shultz, J. Phys. Chem. Lett. **7**, 1945 (2016).
[34] S. Nihonyanagi, S. Yamaguchi, and T. Tahara, J. Chem. Phys. **130**, 204704 (2009).
[35] R. R. Feng, Y. Guo, R. Lü, L. Velarde, and H. F. Wang, J. Phys. Chem. A **115**, 6015 (2011).
[36] R. Superfine, J. Y. Huang, and Y. R. Shen, Opt. Lett. **15**, 1276 (1990).
[37] X. Wei, S. C. Hong, X. Zhuang, T. Goto, and Y. R. Shen, Phys. Rev. E **62**, 5160 (2000).
[38] W. Gan, D. Wu, Z. Zhang, R. R. Feng, and H. F. Wang, J. Chem. Phys. **124**, 114705 (2006).
[39] X. H. Hu, F. Wei, H. Wang, and H. F. Wang, J. Phys. Chem. C **123**, 15071 (2019).
[40] M. Okuno and T. A. Ishibashi, J. Phys. Chem. Lett. **5**, 2874 (2014).
[41] M. Okuno and T. A. Ishibashi, J. Phys. Chem. C **119**, 9947 (2015).
[42] S. J. Byrnes, P. L. Geissler, and Y. R. Shen, Chem. Phys. Lett. **516**, 115 (2011).
[43] X. Zhuang, P. B. Miranda, D. Kim, and Y. R. Shen, Phys. Rev. B **59**, 12632 (1999).
[44] L. Lin, W. Zhou, R. Gao, S. Yao, X. Zhang, W. Xu, S. Zheng, Z. Jiang, Q. Yu, Y. W. Li, C. Shi, X. D. Wen, and D. Ma, Nature **544**, 80 (2017).
[45] R. Zhang, X. Peng, Z. Jiao, T. Luo, C. Zhou, X. Yang, and Z. Ren, J. Chem. Phys. **150**, 074702 (2019).
[46] M. Smits, M. Sovago, G. W. Wurpel, D. Kim, M. Müller, and M. Bonn, J. Phys. Chem. C **111**, 8878 (2007).
[47] J. Tan, Y. Luo, and S. Ye, Chin. J. Chem. Phys. **30**, 671 (2017).
[48] J. Tan, J. Zhang, Y. Luo, and S. Ye, J. Am. Chem. Soc. **141**, 1941 (2019).
[49] S. Yao, X. Zhang, W. Zhou, R. Gao, W. Xu, Y. Ye, L. Lin, X. Wen, P. Liu, B. Chen, E. Crumlin, J. Guo, Z. Zuo, W. Li, J. Xie, L. Lu, C. J. Kiely, L. Gu, C. Shi, J. A. Rodriguez, and D. Ma, Science **357**, 389 (2017).
[50] W. Liu, L. Zhang, and Y. R. Shen, Chem. Phys. Lett. **412**, 206 (2005).

DOI:10.1063/1674-0068/cjcp2303020